

ROLUL ORIENTĂRII STRATELOR DE SEDIMENT ȘI A CONCENTRAȚIEI SĂRURILOR ASUPRA EVOLUȚIEI PROPRIETĂȚILOR PETROFIZICE ALE CALCARENITELOR ÎN TIMPUL CICLURILOR DE DEGRADARE SUB ACȚIUNEA CLORURII DE SODIU ROLE OF SEDIMENT BEDDING ORIENTATION AND SALT CONCENTRATION ON THE EVOLUTION OF PETROPHYSICAL PROPERTIES OF CALCARENITE STONE DURING SALT WEATHERING CYCLES BY SODIUM CHLORIDE

M. HRAITA^{1*}, Y. EL RHAFFARI¹, G. FADILI¹, A. SAMAOUALI¹, Y. GÉRAUD², M. BOUKALOUCH¹

¹Thermodynamics Laboratory, Department of Physics, Faculty of Sciences, Mohammed V University of Rabat, B.P. 1014, Morocco.

²Université de Lorraine, École Nationale Supérieure de Géologie, UMR 7359 Géo-Ressources, Rue du Doyen Marcel Roubault TSA 70605, 54518 Vandoeuvre-lès-Nancy Cedex, France.

The importance of capillary imbibition and evaporation processes in the alteration of building stones under the action of salt crystallization can be estimated by various experimental techniques. The aim of this study is to understand the direct relationships between salt weathering, petrophysical and structural properties. We chose to work on calcarenite stone which was commonly used as building material in historical monuments in Morocco. Laboratory wetting-drying cycles were tested on calcarenite specimens with sodium chloride solutions of different concentrations. Results show that the permeability and specific mass of precipitated salt depend on the material porosity and solution concentration. Moreover, variations of thermal conductivity and permeability during applied cycles are less important for samples taken parallel to the sediment bedding than for those taken perpendicularly. The material anisotropy will also be discussed.

Keywords: Calcarenite stone, Salt weathering, Moroccan historic monuments, Permeability, Thermal conductivity.

1. Introduction

Built heritage is the unique and irreplaceable architecture with historic background that merits preservation for future generations. We are interested in this paper on the calcarenite stone, a material largely used since antiquity by both Romans and Muslims as a building material of historical monuments in the coastal cities in Morocco (e.g. Fig. 1) [1-3]. Given their location on the edge of ocean, these buildings are subjected to significant salt weathering problems [4]. Several studies [3, 5] were carried out on some sites in Rabat city: the citadel of Chellah, the ramparts and the old medina doors. These sites are made up of calcareous stones similar to those which are the subject of our study. The authors studied the surface deterioration of these monuments and showed that the sodium chloride formation (halite) constitutes the main factor of deterioration of these stones.

The crystallization of soluble salts in porous construction materials has been recognized as one of the most important weathering process contributing to the decay of many cultural objects such as wall paintings, sculptures, historic

monuments, and other artworks (e.g. Fig. 2) [4, 6, 7]. These soluble salts penetrate in the porous network primarily by capillarity [8], and then crystallize during an evaporation process [9]. The principal factors influencing salt crystallisation damage in porous materials are related to the properties of rock (resistance to crystallisation pressure, mineralogy, texture and structure) of porous network (pore size distribution, average pore radius and porosity) of salt itself (salt concentration, location of crystallization, crystallization pressure, forms of the crystals) and of environmental conditions (temperature, relative humidity) [4, 10].

Salt crystallizes when the concentration in solution reaches saturation point. According to the conditions, the saturation state can be reached on the surface of porous medium, which give rise to the formation of efflorescence (e.g. NaCl: halite) or on the contrary within the porous medium, leading to the formation of subflorescence (e.g. Na₂SO₄: thenardite/mirabilite) [11]. Indeed, if the advective transport of ions towards surface induced by evaporation is sufficient to cause a peak of concentration at the surface, therefore salt efflorescence will take place. The subflorescence

* Autor corespondent/Corresponding author,
E-mail: simo.hraita@yahoo.fr, mohamed-hraita@hotmail.com



Fig. 1 – Examples of calcarenite historic monuments built in the edge of Atlantic Ocean between Rabat and Kenitra. Left picture: Kasbah of the Udayas located at the mouth of the Bouregreg river in Rabat city. Right picture: Kasbah of Mehdiya situated at the mouth of the Sebou river, about 8 km west of Kenitra city.



Fig. 2 – Walls bases in calcarenite in the garden of Udayas already restored; soil water rises by capillary transfer in the base, contour scaling initiated on the part in contact with the ground in zone (a) where evaporation is faster than capillary rise, development of green algae (zone b) and lichen (zone c), white efflorescence of salts (zone d) where the water evaporates on the surface, (zone e) always wet.

may occur at a later stage of drying if the solution is not hydraulically connected to the surface of the porous medium (phase of drying where the evaporation front is within the porous medium) [12]. Salt subflorescence produces considerably more decay in porous stone than salt efflorescence [11, 13-15].

It is generally accepted that the damage of building stones arises from repeated cycles of crystallization-dissolution of soluble salts within the porous network, because of the impact of such cycles on the ion concentration (formation of supersaturated solutions) [16, 17] and on the structure of the precipitated salt [18]. Different theoretical explanations have been proposed. The most popular ones include the crystallization pressure against the pore walls, hydration pressure, thermal expansion, osmotic pressure, irreversible dilation, and chemical weathering [19-21]. Nevertheless, the mechanism of salt weathering by crystallization pressure appears to be the most relevant [17, 18, 22]. This mechanism was first advanced by Correns in 1949 [23]. In fact, in an under saturated conditions, the crystallization is impossible. The crystals growing into just

saturated conditions cannot exert any crystallization pressure. However, crystals growing into supersaturated conditions can exert a high pressure. If crystals growing into supersaturated conditions are confined in a pore space, it can create enough pressure susceptible to disrupt the porous matrix [21].

Considering the importance of salt weathering in building stones, not only from a geomorphologic point of view, but also from a cultural and economic standpoint [4], it is essential to know the mechanisms of damage and the parameters controlling the process of salt weathering as a first step to design methods to solve, or at least mitigate, this problem in the fields of civil engineering and cultural heritage conservation [4].

In this paper, we have been determined the influence of sediment bedding, porosity and solution concentration on salt precipitation as well as the evolution of permeability and thermal conductivity during wetting-drying cycles. For this purpose, five tests of accelerated aging by crystallization-dissolution cycles are carried out with sodium chloride solutions of different



Fig. 3 – (a) Calcarenite block used for coring eight identical cylindrical samples: (c) four cores taken parallelly to the sediment bedding (series 1) and (d) four other perpendicularly to this one (series 2). (b) Four calcarenite cores between two standard samples positioned along the scanning direction on the platform of thermal conductivity scanner (TCS). The pictures (c) and (d) are taken after the first dissolution-crystallization cycle, and show the NaCl efflorescence formation.

concentrations on calcarenite samples, taken parallelly (series 1) and perpendicularly (series 2) to the sediment bedding. This procedure pretends to experimentally simulate natural alterations in-situ, particularly lower walls of building structures located within the zone of capillary rise of saline groundwater.

2. Experimental

2.1. Calcarenite stone characterization

Calcarenite rock is a coarse bioclastic limestone [5, 24] which corresponds to the coastal Plio-Quaternary sandstone outcropping in a more or less continuous manner between Casablanca and Larache [1, 2, 5, 24]. The samples selected for this study are cored from a calcarenite block (Fig. 3a) of 12 cm side which was extracted from the quarry in Rabat area. Eight identical cylindrical samples of 33 mm in length and 50 mm in diameter have been selected for this study. Four specimens were taken in parallel to the sediment bedding (series 1) (Fig. 3c) and four other perpendiculars with this one (series 2) (Fig. 3d). We chose to work on the same samples of which we already have been determined the petrophysical, structural and mineralogical properties in their original unaltered state [1]. This will help us to better understand the alteration mechanism of calcarenite stone by salt precipitation.

Results obtained in [1] showed that these samples are composed essentially of two major crystalline phases forming their structure: calcite (70.97%) and quartz (6%). They are characterized by a rather high total porosity (between 22.44 and 29.61%), a low trapped porosity (between 2.14 and 4.12%) and a high permeability. Other results (Tab. 1) highlight an initial isotropy of this material according to the bedding orientation with respect to thermal conductivity and permeability.

2.2. Salt crystallisation test

The salt used for this study was sodium chloride (NaCl). This saline mineral is commonly found in building materials and other elements of our cultural heritage, and its main source is linked to sea spray [11]. NaCl is frequently used in salt crystallisation laboratory tests [11, 25]. Under room conditions, the sodium chloride-water system has one stable phase - halite (NaCl) [11].

Salt crystallisation test was performed using an experimental technique inspired from the protocol test No.II.6 of standard RILEM (1978). In order to avoid the evaporation process which may accompany those of capillarity, the samples were placed vertically on a rack, then in a tray closed hermetically by a sealing cover that maintains humidity close to saturation. The saline solution level of about 3 mm is kept constant at the bottom

Table 1

Petrophysical properties of calcarenite cores in unaltered state (cycle n° 0) [1].

	Cores parallel to the sediment bedding (series 1)				Cores perpendicular to the sediment bedding (series 2)			
	EP1	EP2	EP3	EP4	EH1	EH2	EH3	EH4
Water porosity N24 (24 hours)	15.98	16.38	18.27	18.86	19.35	16.31	19.29	17.16
Permeability (Darcy)	2.027	2.291	5.014	7.470	5.785	5.341	6.731	4.201
Thermal conductivity W/(m.K)	1.194	1.150	1.165	1.166	1.188	1.179	1.150	1.151

Table 2

Concentration of sodium chloride solutions used for capillary rise technique.

	Cores parallel to the sediment bedding (series 1)				Cores perpendicular to the sediment bedding (series 2)			
	EP1	EP2	EP3	EP4	EH1	EH2	EH3	EH4
[NaCl] (g/l)	45	15	45	15	45	15	15	45

of the tray throughout all experiment duration performed in an air-conditioned room at 25°C. We considered two different concentrations of NaCl solution - 15 and 45g/l (Table 2). After contamination (saturation), the samples are oven-dried at 60°C for 48 hours until constant dry weight. This procedure is repeated so as to perform five wetting-drying cycles. The permeability and thermal conductivity of each sample were measured after each cycle.

2.3. Characterization techniques

In this paper, we highlight the relationships between salt crystallization (specific mass of precipitated salt), transport properties (permeability, thermal conductivity), and pore structure (porosity, sediment bedding), which are particularly interesting parameters for interpreting salt weathering process. For that, we performed different measurements using different techniques, including thermal conductivity scanner and TinyPerm II portable air permeameter.

Permeability measurements were carried out with the permeameter TinyPerm II, made by New England Research, Inc.. It is a unique hand-held device that can characterize the permeability of rocks and soils or the effective hydraulic aperture of fractures in situ on outcrops as well as on laboratory specimens [26]. The apparatus is capable of making permeability measurements ranging from 0.01 to 10 Darcies for matrices and 10 μm to 2 mm fracture apertures [26]. Although the measurements could have been made in the field, all measurements reported here are made on the specimens in laboratory.

Thermal conductivity analysis was performed using the optical scanning method, developed by Yuri Popov. The device used in this technic is called Thermal Conductivity Scanner (TCS) and comprises a mobile carriage, placed just below the platform on which are arranged the test samples (Fig. 3b). This block has a heat source, on both sides of which are incorporated two sensitive temperature sensors. The advantages of this technic include high speed of operation,

contactless mode of measurement, and the ability to measure directly on a core sample and to estimate the thermal anisotropy and inhomogeneity of rocks. It is an attractive alternative for non-destructive measurements of thermal properties (thermal conductivity and thermal diffusivity) of large numbers of minerals, rocks and ore samples [27].

The theoretical model is based on scanning a sample surface with a focused, mobile and continuously operated heat source in combination with infrared temperature sensors [1, 27]. The heat source and sensors move with the same speed relative to the sample and at a constant distance to each other. The second temperature sensor displays the value of the maximum temperature rise along the heating line behind the source. The maximum temperature rise θ is determined by the relationship:

$$\theta = \frac{Q}{2\pi \cdot x \cdot \lambda}$$

where Q is the source power and x is the distance between source and sensor. The analysed sample is positioned along the scanning direction on the device platform between two identical standard samples (Fig. 3b) with known thermal conductivity λ_R . Thus, the thermal conductivity of the studied sample can be determined from λ_R and the ratio of θ_R to θ . This relation is expressed as:

$$\lambda = \lambda_R \cdot \left(\frac{\theta_R}{\theta} \right)$$

3. Results and discussion

We performed unidirectional wetting-drying cycles along the specimen generatrix. At the end of the drying step, we observed the formation of halite efflorescence on the stone surface, a small quantity of salt remains trapped in the pore space of the stone. The formed salt crust is thin and is not easily detached from the stone surface. These efflorescences accumulate from one cycle to another, especially in the lower part of the sample.

Table 3

Slope values of permeability and specific mass of precipitated salt obtained during wetting-drying cycles (series 1 and 2).

	Cores parallel to the sediment bedding (series 1)				Cores perpendicular to the sediment bedding (series 2)			
	EP1	EP2	EP3	EP4	EH1	EH2	EH3	EH4
Specific mass slope of precipitated salt (10 ⁻³ g/g.cycle)	1.7	0.63	2	0.71	1.82	0.41	0.7	1.88
Permeability slope (Darcy/cycle)	0.081	0.044	0.15	0.070	0.92	0.37	0.43	0.48

Indeed, under the effect of gravity, the fluid transfer occurs from the top to the base of the specimen. The solute diffusion toward the surface is governed by Fick's law. When water saturating partially the stone pores network evaporates, the concentration of solution in pores increases. The salt concentration becomes important and reaches the critical saturation concentration at the specimen surface. So the salt crystallizes by efflorescences formation at the end of drying.

3.1. Specific mass of precipitated salt

The specific mass measurements of the precipitated halite were performed on the samples taken parallelly (series 1) and perpendicularly (series 2) to the sediment bedding. The considered value for each sample is the precipitated salt mass on the sample mass.

Figure 4 shows that the quantity of precipitated salt within the porous network depends closely on the solution concentration and material porosity N24. In fact, the imbibition-drying tests with the same sodium chloride concentration (45g/l) on cores of different porosities show that the specific mass slope of the precipitated salt is more important for higher porosity values (EP3 and EP1) (Tab. 3). Tests carried out on cores of the same porosity, show that the amount of precipitated salt increases with the sodium chloride concentration (EH3 and EH1) (Table 3).

3.2. Permeability

The permeability value is the average of the values obtained on each side of the core. In unaltered state, the permeability of different samples (series 1 and 2) is between 2.03 and 7.47 *Darcies* and demonstrates the great ability of calcarenite stone for the fluids transport [1]. This can be explained by the absence of clay grains in the stone structure, by the important values of total porosity, macroporosity and threshold pore access diameter [1]. The dispersion of permeability values is mainly due to the rock heterogeneity [1]. After five tests of accelerated aging by crystallization-dissolution cycles, the permeability has undergone a decrease and varies between 1.57 and 6.17 *Darcies* (Fig. 5). This variation can be explained by the presence of salt in the porous system which decreases the porosity. Table 3 presents the slopes of permeability in absolute values according to the number of applied cycles. It shows that the permeability depends considerably on the solution concentration and porosity. Thus, measurements performed with the same NaCl concentration (45g/l), on cores of different porosities (EH1 - 19.35% and EH4 - 17.16%), show that the slope is important for high porosity values. In addition, tests carried out on specimens of same porosity (EH1 - 19.35% and EH3 - 19.29%), show that the permeability decreases considerably during the applied cycles when the solution concentration increases.

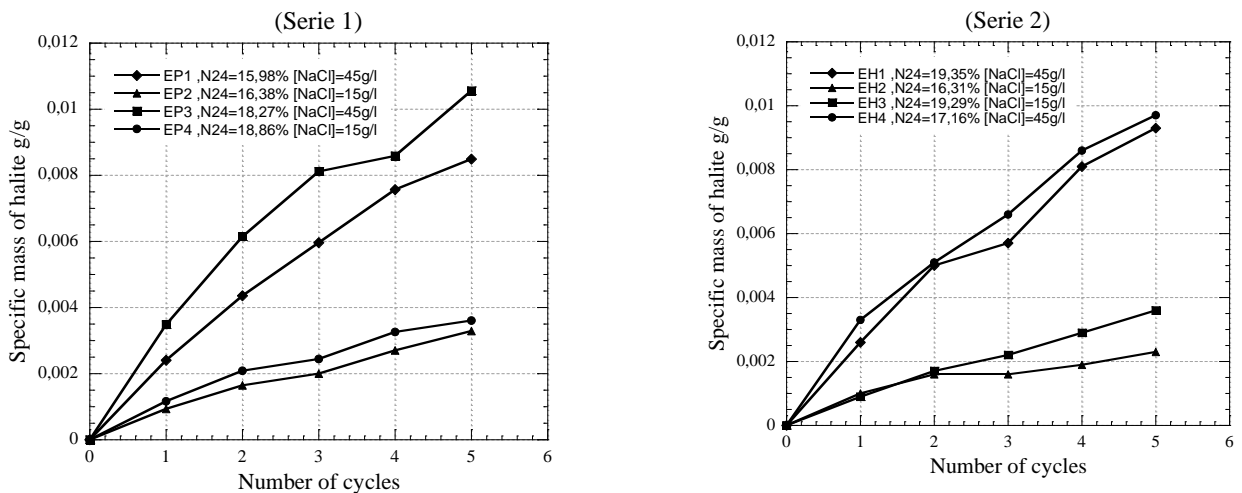


Fig. 4 – Evolution of specific mass of precipitated halite during crystallization-dissolution cycles.

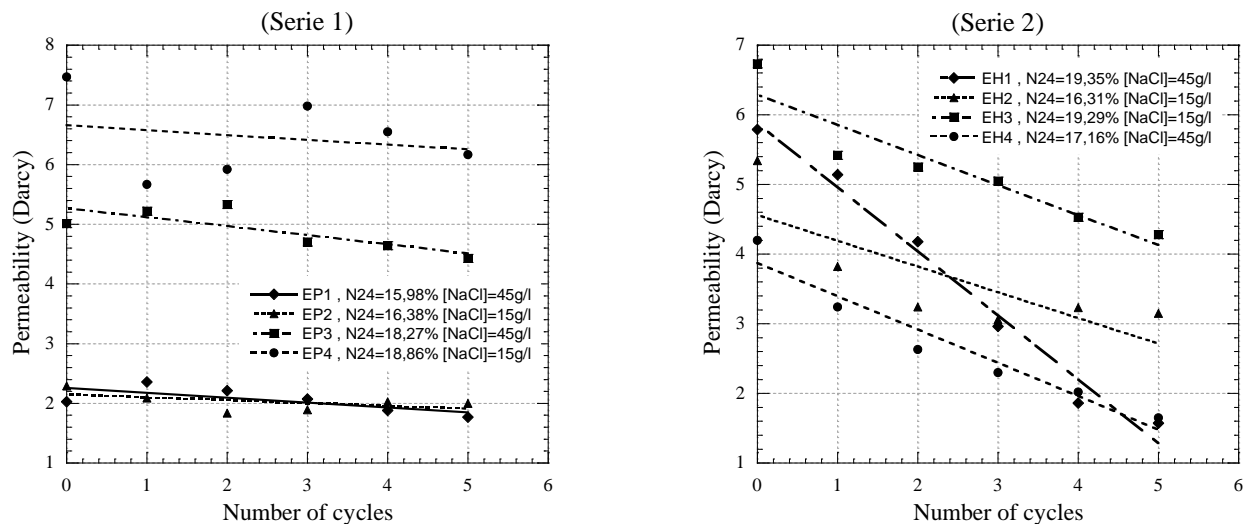


Fig. 5 - Evolution of permeability of calcarenite samples (series 1 and 2) during salt weathering cycles.

Figure 5 also shows that the decrease in permeability during wetting-drying cycles is less important for cores taken parallelly to the sediment bedding (Series 1) than for those taken perpendicularly (series 2). Slope values are indeed between 0.044 and 0.15 for series 1 and between 0.37 and 0.92 for series 2 (Tab. 3). Consequently, the influence of salt weathering cycles on calcarenite stone is controlled by the fluid flow direction (parallel or perpendicular to the sediment bedding), the solution concentration and the porosity.

3.3. Thermal conductivity

Thermal conductivity of a building material (stone, rock, concrete) depends closely on its porosity and mineralogy; these two characteristic parameters of material evolve with its alteration [3]. The thermal conductivity measurement can thus be used to characterize the material alteration. Indeed, the daily and seasonal variations in ambient temperature create thermal cycles which can be at the origin of the stone alteration. If conductivity is low, the temperature of the surface of the stone increases more quickly with respect to its subjacent part, which generates considerable thermal gradients. On the other hand, a high conductivity promotes the absorption of solar irradiation and attenuates the temperature variations between the surface and the sub-surface of the stone [28].

TCS method allows to determine the thermal conductivity of the surface sample [27]. The samples are covered with black paint to avoid parasitic reflections due to the sample colour. Measurements are performed along a profile on the sample surface. We considered two profiles, the first according to the core generatrix, and two others according to base diameters. Thermal conductivity is then determined as an average value of local thermal conductivities measured along the

profile; the error is about 2% [27]. The main minerals constituting the calcarenite stone are the quartz and the calcite; the average thermal conductivities of these minerals found in literature are $\lambda_{\text{quartz}} = 7,69 \text{ W.m}^{-1}.\text{K}^{-1}$ [29] and $\lambda_{\text{calcite}} = 3,59 \text{ W.m}^{-1}.\text{K}^{-1}$ [30] respectively.

Figure 6 presents the average thermal conductivity profiles during the imbibition-drying cycles. On healthy cores, the values are between 0.97 and 1.1 $\text{W.m}^{-1}.\text{K}^{-1}$ for the profiles performed along the generatrix, and between 1.25 and 1.36 $\text{W.m}^{-1}.\text{K}^{-1}$ for profiles carried out according to the diameters. Notable variations of thermal conductivity observed in the set of the studied profiles, are significant of an initial heterogeneity of the material structure [1]. After five tests of accelerated aging by crystallization-dissolution cycles, the values are between 1.07 and 1.12 $\text{W.m}^{-1}.\text{K}^{-1}$ for generatrix, and between 1.25 and 1.40 $\text{W.m}^{-1}.\text{K}^{-1}$ for core diameters. This increase in thermal conductivity does not seem to evolve considerably with the precipitated salt quantity, but it indicates the presence of salt in porous network and thus a reduction in porosity. In fact, the salt which fills the pores has a greater conductivity than that of air.

Figure 6 also shows that the impact on thermal conductivity, by imbibition-drying cycles under salt crystallization action, is less important for cores taken parallelly to the sediment bedding than for those taken perpendicularly. These results are consistent with those of permeability and show that the capillary rise direction controls the material damage.

The results presented in Figure 7 indicates that the thermal conductivity decreases when the porosity increases; this result is in good agreement with that found by Y. El Rhaffari [2]. The high thermal conductivity values correspond to low porosity regions testifying to the existence of a calcite and quartz cementation and vice versa.

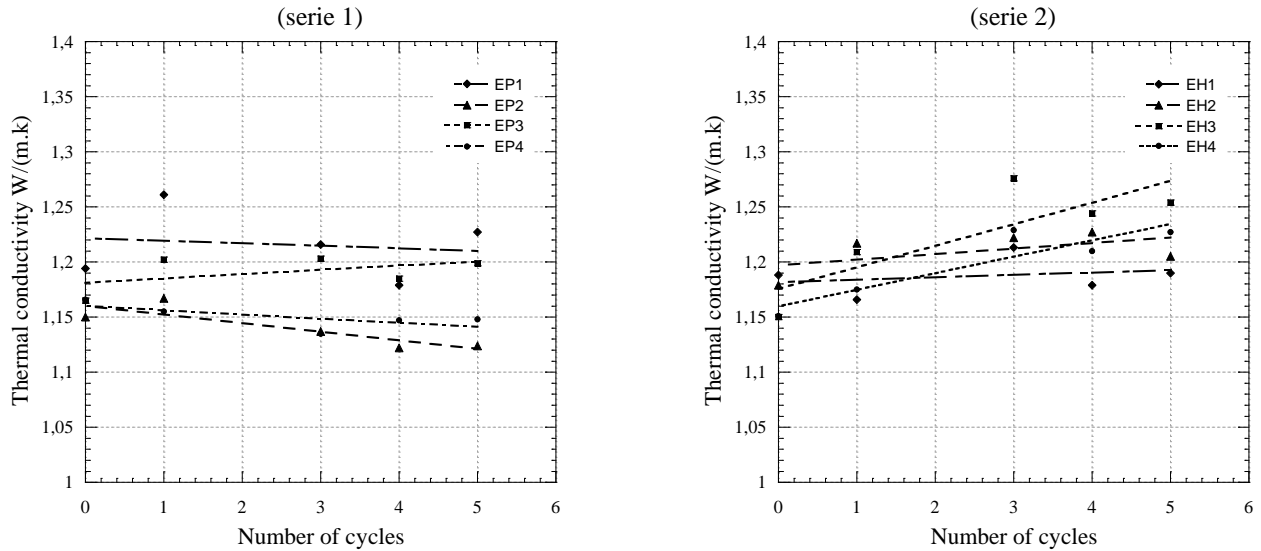


Fig. 6 - Evolution of average thermal conductivity for calcarenite samples (series 1 and 2) during salt weathering cycles by imbibition-drying.

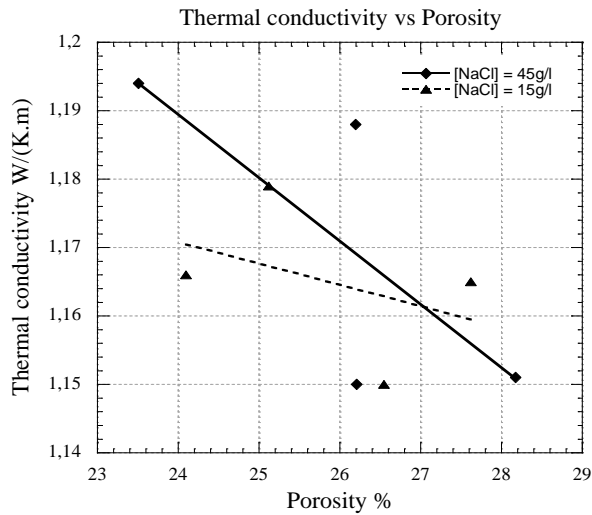


Fig. 7 - The thermal conductivity in function of porosity for four samples tested with sodium chloride solution of 15 g/l and four others with 45g/l.

Calcarenite stone in the *unaltered* state presents an initial isotropy according to the bedding orientation with respect to thermal conductivity and permeability [1] (Table 1). However, these properties evolve anisotropically during applied cycles. This can be attributed to differences in the orientations and structures of specific pore network at each sampling direction (parallel and perpendicular to the bedding). We can say that the anisotropy of the transfer properties in calcarenite rock (evaporation, thermal conductivity, permeability ...) is characteristic of the anisotropy of structure and pore network connectivity.

4. Conclusions

This paper presents the study at a macro scale of salt weathering in calcarenite stone using

different techniques, including *thermal conductivity scanner* and *Tiny Perm II permeameter*. Several imbibition-drying cycles are carried out in laboratory with sodium chloride solutions, on eight calcarenite samples taken parallel and perpendicular to the sediment bedding. Changes noticed for a few number of applied cycles are more important when a low NaCl concentration solution was used. We observed the formation of salt efflorescence on sample surface, the minor part of halite remaining trapped in stone porous network. These efflorescences have caused significant changes in the texture and structure of tested specimens, these results in the decrease of permeability with the applied cycles.

Results show that the bedding orientation represents a primary factor in calcarenite stone decay under salt crystallization action. The evolution of permeability and of the specific mass of precipitated salt depend on salt solution concentration and of porosity. The variations of thermal conductivity and permeability during the imbibition-drying cycles are less important for samples taken parallel to the sediment bedding than for those taken perpendicularly. However, the limited number of applied cycles did not allow showing the effect of salt concentration difference on thermal conductivity.

Results also showed that the thermal conductivity decreases when the porosity increases. In addition, calcarenite stone in the *unaltered* state presents an initial isotropy according to the bedding orientation with respect to thermal conductivity and permeability. However, these properties evolve anisotropically during applied cycles.

We plan in perspective to study the petrophysical, petrographical, mineralogical and structural properties of altered calcarenite stone by

salt crystallization. This study will relate to the same samples, of series 1 and 2, subjected to the salt weathering action during the five imbibition-drying cycles which we have performed.

Acknowledgements

This work was supported by the French-Moroccan cooperation within the project named (PAI-Volubilis) No. MA/07/168, between Louis Pasteur University of Strasbourg and Mohammed V University of Rabat.

REFERENCES

1. M. Hraïta, Y. El Rhaffari, A. Samaouali, Y. Géraud and M. Boukalouch, Petrophysical, petrographical and mineralogical characterization of calcarenite rock used for monumental building in Morocco, Romanian Journal of Materials 2014, **44**(4), 365.
2. Y. El Rhaffari, M. Hraïta , A. Samaouali, M. Boukalouch and Y. Géraud, Thermal and petrophysical characteristics of calcarenite rocks used in the construction of monuments of Rabat, Romanian Journal of Materials 2014, **44**(2), 153.
3. A. Samaouali, L. Laânab, M. Boukalouch and Y. Géraud, Porosity and mineralogy evolution during the decay process involved in the Chellah monument stones, Environ Earth Sci, 2010, **59**, 1171-1181. DOI: 10.1007/s12665-009-0106-5.
4. C. Cardell, F. Delalieux, K. Roumpopoulos, A. Moropoulou, F. Auger and R. Van Grieken, Salt-induced decay in calcareous stone monuments and buildings in a marine environment in SW France. Construction and Building Materials 2003, **17**, 165.
5. N. Zaouia, M. EL wartiti and B. Baghdad, Superficial alteration and soluble salts in the calcarenite weathering. Case study of almohade monument in Rabat: Morocco. Environ. Geol., 2005, **48**, 742.
6. D. Benavente, J. Martínez-Martínez, N. Cueto and M.A. García-del-Cura, Salt weathering in dual-porosity building dolostones, Engineering Geology 2007, **94**, 215.
7. C. Cardell, D. Benavente and J. Rodríguez-Gordillo, Weathering of limestone building material by mixed sulfate solutions. Characterization of stone microstructure, reaction products and decay forms, Materials Characterization 2008, **59**, 1371.
8. M. Angelie, PhD thesis, Multiscale study of stone decay by salt crystallization in porous networks, Université de Cergy-Pontoise, Laboratoire de tectonique UMR 7072. 2007.
9. N. Sghaier, PhD thesis, Evaporation en milieu poreux en présence de sel dissous. Influence des films liquides et des conditions de mouillabilité, Institut de Mécanique des Fluides de Toulouse, France 2006.
10. D. Benavente, N. Cueto, J. Martínez-Martínez, M. A. García del Cura and J. C. Canaveras, The influence of petrophysical properties on the salt weathering of porous building rocks, Environ Geol 2007, **52**, 215-224. DOI: 10.1007/s00254-006-0475-y.
11. D. Benavente, M.A. Garcia del Cura, J. Garcia Guinea, S. Sanchez-Moral and S. Ordoñez, Role of pore structure in salt crystallisation in unsaturated porous stone, Journal of Crystal Growth 2004, **260**, 532.
12. N. Sghaier, M. Prat and S. Ben Nasrallah, Efflorescence chou-fleur, efflorescence croûte et leur impact sur l'évaporation d'un milieu poreux, 21 ème Congrès Français de Mécanique – Bordeaux, 2013.
13. E.M. Winkler, Stone in Architecture: Properties, Durability, 3rd Edition. Springer-Verlag, Berlin, 1997.
14. C. Rodríguez-Navarro, E. Doehne, Salt weathering: Influence of evaporation rate, supersaturation and crystallization pattern, Earth Surface Processes and Landforms 1999, **24**, 191.
15. C.A. Price, An expert chemical model for determining the environmental conditions needed to prevent damage in porous materials, European commission research report 11, protection and conservation of european cultural heritage, Archetype Publications Ltd. London, 2000.
16. A.S. Goudie, H. Viles, Salt Weathering Hazards, Chichester: John Wiley and Sons Ltd. 1997, 241p.
17. O. Coussy, Deformation and stress from in-pore drying-induced crystallization of salt, Journal of the Mechanics and Physics of Solids 2006, **54**, 1517.
18. G. W. Scherer, Stress from crystallization of salt, Cement and Concrete Research 2004, **34**, 1613.
19. C. Rodríguez-Navarro, L. Linares-Fernandez, E. Doehne and E. Sebastian, Effects of ferrocyanide ions on NaCl crystallization in porous stone, Journal of Crystal Growth 2002, **243**(3-4) 503-516. DOI: 10.1016/S0022-0248(02)01499-9.
20. B. Lubelli, R.P.J. van Hees and C.J.W.P. Groot, Sodium chloride crystallization in a "salt transporting" restoration plaster, Cement and Concrete Research 2006, **36**, 1467.
21. N. Thaulow and S. Sahu, Mechanism of concrete deterioration due to salt crystallization, Materials Characterization 2004, **53**, 123.
22. C. Rodríguez-Navarro, E. Doehne and E. Sebastian, How does sodium sulfate crystallize? Implications for the decay and testing of building materials, Cement and Concrete Research 2000, **30**, 1527.
23. C.W. Correns, Growth and dissolution of crystals under linear pressure, Discussions of the Faraday Society, London 1949, **5**, 267.
24. H. Azouaoui, N. El Hatimi and N. El Yamine, Plio-Quaternary formations of the Casablanca area (Morocco): sedimentological and geotechnical aspects, Bull Eng Geol Environ, 2000, **59**, 59.
25. A.S. Goudie, Salt weathering simulation using a single-immersion technique, Earth Surface Processes and Landforms 1993, **18**, 368.
26. A. Rahmouni, A. Boulanouar, M. Boukalouch, Y. Géraud, A. Samaouali, M. Harnafi and Jamal Sebbani, Relationships between porosity and permeability of calcarenite rocks based on laboratory measurements, J. Mater. Environ. Sci. 2014, **5**(3), 931.
27. Y. A. Popov, D. Pribnow, J.H. Sass, C.F. Williams and H. Burkhardt, Characterization of rock thermal conductivity by high-resolution optical scanning, Geothermics, 1999, **28**, 253.
28. A. Samaouali, PhD thesis, processus d'altération et transfert de fluides dans les pierres calcarénites du monument chellah-Rabat, Mohammed V university of Rabat, Morocco, 2011.
29. Y. Guégen, V. Palciauskas, Introduction à la physique des roches. Hermann Ed., 1992, 299 pp.
30. K. Horai, Thermal conductivity of rock-forming minerals, J. Geoph. Res. 1971, **26**, 1278.
